

# Controllable Synthesis of Upconversion Nanophosphors toward Scale-Up Productions

Yiran Jiao, Chen Ling, Jie-Xin Wang, Honeyfer Amanico, Joshua Saczek, Haoyu Wang, Sreepathy Sridhar, Ben Bin Xu,\* Steven Wang,\* and Dan Wang\*

Upconversion nanophosphors (UCNPs) are considered as an important synthesis arm within biomedical and energy sectors due to their unique optical characteristics, which can convert near-infrared light into higher energy emissions. However, key challenges, cost, compatibility of the materials, etc. have to be taken into serious consideration to transform this in-lab UCNPs technology into scale-up production for wider commercial needs. This review highlights the fundamental concepts of synthetic approaches for UCNPs and recaps recent advances in terms of large-scale production. A number of typical synthesis routes in both batch and continuous processes are reviewed, alongside their limitations and potential improvements when being considered for mass production. By discussing and exploiting the technical compacity for the potential synthetic trends, key challenges, and expectations of future synthesis methods for UCNPs are also outlined.

## 1. Introduction

Luminescence is a physical process to transform external stimuli into light emission, where these external stimuli can be light or other electromagnetic radiation. This phenomenon can be found in a variety of materials including organic dyes,<sup>[1]</sup> semiconductor quantum dots,<sup>[2]</sup> noble metal nanoclusters,<sup>[3]</sup> and lanthanide-doped phosphors.<sup>[4,5]</sup> In the last few years, the development of lanthanide-doped materials has attracted considerable interests due to their unique optical properties,<sup>[6]</sup> especially upconversion properties.<sup>[7]</sup>

The upconversion scheme, first proposed by Bloembergen<sup>[8]</sup> (1959) and demonstrated by Porter<sup>[9]</sup> (1961), represented

an alternative to traditional Stokes photoluminescence, where it can convert near-infrared (NIR) light into ultraviolet (UV), visible, or NIR light,<sup>[10]</sup> enabling deeper penetration into biological tissues.<sup>[11]</sup> This feature together with its low toxicity, low auto-fluorescence, and high resistance to photobleaching<sup>[6,12–15]</sup> allows upconversion nanomaterials to be attractive carriers in downstream applications including in vitro and in vivo bioimaging,<sup>[16]</sup> drug delivery,<sup>[17]</sup> solar cells,<sup>[18]</sup> and photoreactions.<sup>[19]</sup>

Classical upconversion luminescence originates from upconversion nanoparticles (UCNPs), especially rare earth-doped UCNPs, which consists of a host matrix and dopant ions. A typical rare earth-doped UCNPs luminescent system is illustrated in **Figure 1**. Usually, dopant ions serve as luminescent activators and sensitizers.<sup>[20]</sup> By properly choosing the emission bands of doping ions, desired emission bands from UV to NIR can be achieved.<sup>[21,22]</sup> The host matrix could also act as a platform for upconversion emission<sup>[23]</sup> wherein the size, morphology, and phase of the host matrix can influence the performance of dopant ions and the corresponding upconversion luminescent intensity.<sup>[24,25]</sup> For example, it is found that in general when the NaREF<sub>4</sub> UCNPs size decreases, the emission intensity decreases as well. This is induced by the nonradiative relaxation of energy transfer and the quenching effect of surface ligands.<sup>[26]</sup>

Even though the relationship between optical performance and morphology of UCNPs have had been well understood,<sup>[23–26]</sup> relevant developments on commercializing such nanomaterials are hampered due to scaling-up production process, where bottlenecks normally exist in the reproducibility, repeatability as well as the yield from these methods. By recapping these reported synthesis methods, for example, thermal decomposition,<sup>[35–40]</sup> co-precipitation,<sup>[60–66]</sup> hydrothermal,<sup>[73–78]</sup> and ion exchange,<sup>[98–101]</sup>

Y. Jiao, Prof. J.-X. Wang, Prof. D. Wang  
State Key Laboratory of Organic Inorganic Composites  
Beijing University of Chemical Technology  
Beijing 100029, China  
E-mail: wangdan@mail.buct.edu.cn

Y. Jiao, Prof. J.-X. Wang, Prof. D. Wang  
Research Centre of the Ministry of Education for High Gravity  
Engineering and Technology  
Beijing University of Chemical Technology  
Beijing 100029, China


C. Ling, Dr. S. Wang  
Department of Mechanical Engineering  
City University of Hong Kong  
Hong Kong 999077, China  
E-mail: steven.wang@cityu.edu.hk

H. Amanico  
Department of Chemical Engineering and Biotechnology  
University of Cambridge  
Cambridge CB2 3RA, UK

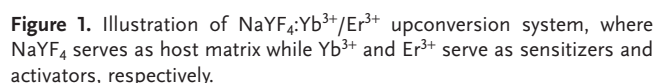
J. Saczek  
School of Engineering  
Newcastle University  
Newcastle upon Tyne NE1 7RU, UK

Dr. H. Wang  
Department of Chemical Engineering  
Imperial College London  
London SW7 2AZ, UK

S. Sridhar, Prof. B. B. Xu  
Department of Mechanical and Construction Engineering  
Faculty of Engineering and Environment  
Northumbria University  
Newcastle upon Tyne NE1 8ST, UK  
E-mail: ben.xu@northumbria.ac.uk

 The ORCID identification number(s) for the author(s) of this article can be found under <https://doi.org/10.1002/ppsc.202000129>.

DOI: 10.1002/ppsc.202000129



in lab,<sup>[27,28]</sup> and the scale-up process where the breaking of local thermodynamic equilibrium is likely to occur to yield the uncontrollable changes on the phases and other features for the particle, especially the luminescent performance.<sup>[29,30]</sup> Despite the understanding on the nucleation mechanism of UCNPs obtained through complicated synthesis, there is little focused discussion on the large-scale industrial production of UCNPs.

In this article, we distinguish the synthesis approaches into batch and continuous process, according to the preparation route. The continuous process includes uninterrupted kinetical processing as well as continuous flow stream down to the reactor outlet, while batch process largely involves pot-by-pot production. A general overview of the methods classification is presented in **Table 1**. We first review the traditional UCNP synthesis processes in batch reactors along with their reaction mechanisms, at the same time looking at the potential scale-up synthesis approaches. Various factors including fabrication requirements, environmentally friendly reagents, and by-products are presented and studied. Additionally, popular continuous preparation methods, for example, process intensification technologies and continuous flow reactors, are featured and thoroughly reviewed as they have the potential to be embedded into industrial processes and will be expected to enhance yield and efficiency of the synthesis process. Attempts are made to outline the existing challenges and the future scalable production of UCNPs.

Types of reactor	Reaction strategy	Advantages	Disadvantages	Precursors	Product obtained	Reaction conditions	Ref.
Batch reactor	Thermal decomposition	Rapid synthesis, simple operation	Expensive and air-sensitive precursors, toxic by-product, cost inefficient	$\text{RE}(\text{CF}_3\text{COO})_3$	$\text{LaF}_3$	280 °C for 1 h under Ar	[35]
					$\text{NaYF}_4$	300 °C for 1 h under Ar	[36]
					$\text{LiYF}_4$	—	[37]
					$\text{NaGdF}_4$	310 °C for 1 h under Ar	[38]
					$\text{NaYbF}_4$	310 °C for 1 h under Ar	[39]
					$\text{Sr}_2\text{YF}_7$	300 °C for 30 min under $\text{N}_2$	[39]
					$\text{LaOBr}$	310 °C for 60 min under $\text{N}_2$	[40]
					$\text{NaYF}_4$	300 C for 60 min under $\text{N}_2$	[60]
					$\text{NaLuF}_4$	300 °C for 2 h under Ar	[61]
					$\text{LiYF}_4$	300 °C for 90 min under $\text{N}_2$	[62]
	Co-precipitation	Inexpensive and nontoxic reagent, harmless by-product	High temperature and inert atmosphere involvement	$\text{RECl}_3$	$\text{KLu}_2\text{F}_7$	150 °C for 60 min under $\text{N}_2$	[63]
					$\text{NaGdF}_4$	280 °C for 2 h under Ar	[64]
					$\text{NaYbF}_4$	320 °C for 30 min under $\text{N}_2$	[65]
					$\text{LiYbF}_4$	320 °C for 60 min under $\text{N}_2$	[66]
				$\text{RE}(\text{Ac})_3$	$\text{Gd}_2\text{O}_3$	180 °C for 24 h	[73]
					$\text{Y}_2\text{O}_3$	180 °C for 60 h	[74]
					$\text{ZnMoO}_4$	—	[75]
					$\text{LaVO}_4$	180 °C for 12 h	[76]
	Hydrothermal	Facile operation, cost efficient	Limited production capacity, long reaction time, high pressure involvement	$\text{RE}(\text{NO}_3)_3 \cdot n\text{H}_2\text{O}$	$\text{NaLuF}_4$	180 °C for 12 h	[77]
					$\text{Sr}_2\text{ScF}_7$	220 °C for 24 h	[78]
				$\text{RECl}_3$	$\text{Y}_2\text{O}_3$	180 °C for 60 h	[74]
					$\text{ZnMoO}_4$	—	[75]

**Table 1.** Continued.

Types of reactor	Reaction strategy	Advantages	Disadvantages	Precursors	Product obtained	Reaction conditions	Ref.
Continuous reactor	Ion exchange	Accurate control on particles size and morphology	Limited options for precursors, complex synthesis steps	RE(OH) <sub>3</sub>	NaREF <sub>4</sub>	120 °C for 12 h	[98]
				Y(OH) <sub>3</sub> F <sub>3-x</sub>	NaYF <sub>4</sub>	180 °C for 18 h	[99]
				ZrOCl <sub>2</sub> ·8H <sub>2</sub> O	Na <sub>3</sub> ZrF <sub>7</sub>	130 °C for 12 h	[100]
				Y <sub>2</sub> (OH) <sub>5</sub> NO <sub>3</sub> ·nH <sub>2</sub> O	NaYF <sub>4</sub>	50 °C for several minutes	[101]
	Microfluidics	Reproducible, homogenous temperature and reagent distribution, crystallization promoted	High temperature and pressure involvement	RE(NO <sub>3</sub> ) <sub>3</sub> ·nH <sub>2</sub> O	LaPO <sub>4</sub> /LaF <sub>3</sub>	110 °C for 20 s (residence time)	[116,117]
				RECl <sub>3</sub>	NaGdF <sub>4</sub>	260 °C, 30 bar for 30 min (residence time)	[104]
				RE(NO <sub>3</sub> ) <sub>3</sub> ·nH <sub>2</sub> O	Gd <sub>2</sub> O <sub>3</sub>	2000 rpm mixing for 15 min, followed by 90 °C for 2 h	[131]
	High gravity	Reproducible, higher mixing efficiency, smaller size distribution for easier scale up	Specialized reactor and additional operation needed	RECl <sub>3</sub>	NaYF <sub>4</sub>	Mixing for 15 min under high gravity, followed by 200 °C for 2 h	[134]
				REF <sub>3</sub>	NaYF <sub>4</sub>	Ball milling for 4 h	[137]
				SrCl <sub>2</sub> , REF <sub>3</sub> RE <sub>2</sub> O <sub>3</sub>	SrFCl Y <sub>3</sub> Al <sub>5</sub> O <sub>12</sub>	Ball milling for 4 h Ball milling for 50 min, repeating for 100 times	[139] [140]

## 2. Synthesis Approaches in Batch Reactors

Batch reactors are commonly used for the synthesis of nanoparticles via different routes. It is widely exercised to use batch synthesis route to achieve controllable nanoparticle characteristics with different capping ligands and operating conditions.<sup>[31–33]</sup> Typical scale-up approaches based on batch production process include thermal decomposition, co-precipitation, hydrothermal, and ion exchange. A general overview of large-scale preparation strategies of UCNPs in batch reactors are presented in **Table 2**.

### 2.1. Thermal Decomposition

Thermal decomposition is a well-developed approach to synthesize UCNPs, which mainly uses rare earth fluoride, trifluoroacetate, etc. as common precursors. These precursors decompose under high temperatures, generally above 300 °C, in a mixed solution of oleic acid (OA), oleylamine (OM), and 1-octadecane (ODE). In this instance, ODE provides the high-temperature decomposition environment while OA and OM serve as capping ligands to regulate particle growth and reduce aggregation.<sup>[34,43]</sup> This method was first utilized by Yan et al. (2005) in

**Table 2.** Several feasible large-scale UCNP synthesis processes in recent years alongside with the morphology, size, luminescent intensity, and weight information of the products.

Synthesis approach	Product	Morphology	Size	Reaction conditions	Luminescent intensity	Product weight	Ref.
Thermal decomposition	NaYF <sub>4</sub> :Yb <sup>3+</sup> ,Tm <sup>3+</sup>	Nanoparticle	—	60.3 mmol RE-OA precursors 115 °C for 1.5 h and then 310 °C for 2 h	Quantum yield at ≈0.14% under power density of 10.0W cm <sup>-2</sup> with NaYF <sub>4</sub> :Yb/Er core	≈10 g	[51]
Solid–liquid thermal decomposition	β-NaGdF <sub>4</sub> :Yb <sup>3+</sup> ,Er <sup>3+</sup>	Nanoparticle	23.5 ± 1.5 nm	200 mmol RE (CH <sub>3</sub> COO) <sub>3</sub> precursors 10 mmol NaHF <sub>2</sub> 250 °C for 30 min and then 310 °C for 30 min	Comparable to counterparts synthesized at 1 mmol	63.38 g with β-NaGdF <sub>4</sub> :Yb, Er@NaYF <sub>4</sub>	[52]
Modified co-precipitation	β-NaYF <sub>4</sub> :Yb <sup>3+</sup> ,Er <sup>3+</sup>	Nanoparticle	22.7 ± 0.7 nm	≈320 °C until upconversion luminescent become visible then cooling down to 200 °C	Quantum yield at ≈0.35% under power density of 150.0W cm <sup>-2</sup> with oleate coated	≈2 g	[69]
Hydrothermal	β-NaYF <sub>4</sub> :Yb <sup>3+</sup> ,Tm <sup>3+</sup>	Micro-plates	Up to 1.125 μm × 0.88 μm	Stirring for 30 min, followed by 180 °C for 6 h	—	≈0.5 g	[94]

**Table 3.** Several UCNP synthesis process toward ultra-small upconversion nanoparticles alongside with the size and luminescent intensity information of the products in recent years.

Synthesis protocols	Product	Size	Notes	Luminescent intensity	Ref.
Gd <sup>3+</sup> doping	$\beta$ -NaGdF <sub>4</sub> :Yb,Er	Down to 6.8 nm	Combination between hydrothermal and thermal decomposition	Stronger emission with NaYF <sub>4</sub> shell	[54]
	NaGdF <sub>4</sub> :Yb,Tm	2.5 ± 0.3 nm	Size ranging from 2.5 to 8.0 nm achieved by varying reaction temperature and time	—	[58]
	NaLuF <sub>4</sub> :Gd,Yb,Er	≈4 nm	Cubic NaGdF <sub>4</sub> as core materials, while inert NaLuF <sub>4</sub> as shell	Colloidal solution visible to eyes	[59]
$\alpha$ -phase particles as precursors	$\beta$ -NaYF <sub>4</sub> :Yb,Er	≈6 nm	Purified $\alpha$ -phase particles redispersed in fresh solvent to convert into $\beta$ -phase	—	[32]
Altering experiments conditions	$\beta$ -NaYF <sub>4</sub> :Yb,Er	≈5 nm	Larger Na/Y ratio favoring $\beta$ -phase particle with smaller size	2 nm thick shell increasing the upconversion efficiency by a factor of 160, while still 1000 times lower than bulk materials	[50]
	NaYbF <sub>4</sub>	≈7 nm	Employing $\alpha$ -phase particles as shell precursors	400 times enhancement of ultraviolet emission with 2 nm NaYF <sub>4</sub> shell doping	[55]
	NaREF <sub>4</sub> (RE = La, Ce, Pr, and Nd)	5–7 nm	Applying oleylamine (OM) for $\beta$ -phase formation	—	[56]
	NaYF <sub>4</sub>	5 nm	Ideal Y <sup>3+</sup> to F <sup>−</sup> ratio at 1:4 2 nm shell of un-doped NaYF <sub>4</sub>	Brighter than 37 nm NaYF <sub>4</sub> core materials	[57]

the synthesis of LaF<sub>3</sub> triangular nanoplates.<sup>[35]</sup> It was then successfully adopted in the preparation of NaREF<sub>4</sub> from lanthanide oxides and trifluoroacetic acid, using lanthanide trifluoroacetate as precursors.<sup>[36]</sup> Currently, this synthesis method has been successfully adopted into various preparation processes for a wide range of UCNPs, including LiYF<sub>4</sub>,<sup>[37]</sup> NaGdF<sub>4</sub>,<sup>[38]</sup> Sr<sub>2</sub>YF<sub>7</sub>,<sup>[39]</sup> and LaOBr.<sup>[40]</sup> The synthesis approach used includes four stages.<sup>[41]</sup> In the first stage, CF<sub>3</sub>COO<sup>−</sup> dissolves, followed by delayed nucleation. The second stage includes the anisotropic growth of the particles. Whereas in stage three, any small particles with less thermodynamical stability redissolve and any large stable particles continue to grow, known as the Ostwald ripening.<sup>[32,42]</sup> Finally, in stage four, aggregates form into various morphologies. During these stages, by simply varying different experimental conditions such as temperature, Na<sup>+</sup>/RE<sup>3+</sup> ratios, OA/OM ratios, and reaction time, nanocrystals with different morphologies and phases can be obtained.<sup>[26,43]</sup>

Compared with other widely used methods, one of the advantages of thermal decomposition is the possibility to synthesize ultra-small upconversion nanoparticles in a relatively simple way, which is highly preferable for their applications.<sup>[44–46]</sup> Particularly, for applications as diagnostic imaging agents, nanoparticles with hydrodynamic diameter under 5.5 nm is ideal to introduce rapid renal clearance, triggering a quick equilibrium between agents injected intravenously and the extracellular space.<sup>[47,48]</sup> While other approaches, such as isolating intermediate  $\alpha$ -NaYF<sub>4</sub> nanoparticles from the reaction solvent followed by redispersing them into fresh solvent with different contents to collect ultra-small  $\beta$ -NaYF<sub>4</sub> particles, or applying additional Gd<sup>3+</sup> doping are also available but require complex operations and result in upconversion emission quenching.<sup>[32,49]</sup> An alternative method based on thermal decomposition developed by Haase et al. (2016) showed a simple method by altering the Na/RE ratio to reduce the obtained UCNPs diameter to 5 nm. A high concentration ratio of Na/RE ions favors  $\beta$ -NaYF<sub>4</sub> seed nucleation, thereby through increasing the sodium oleate ratio in the thermal decomposition process, nanoparticles of

$\beta$ -NaYF<sub>4</sub>, Yb, Er under 5 nm could be achieved.<sup>[50]</sup> Several demonstrated strategies toward ultra-small upconversion nanoparticles' preparation in recent years have been summarized in **Table 3**.

Owing to these unique characteristics, numerous investigations have been devoted to increase the quantity of UCNPs synthesized using thermal decomposition. Zhang et al. (2019) described a high throughput method to synthesize NaYF<sub>4</sub> nanocrystals in one vessel by using liquid RE-OA precursors and increasing the reaction volume with prolonging reaction time. About 10 g of high-quality NaYF<sub>4</sub> nanoparticles could be obtained in one batch with a yield of 678% recorded.<sup>[51]</sup> You et al. (2018) proposed a solid-liquid thermal-decomposition (SLTD) method based on traditional thermal decomposition, **Figure 2**. By using NaHF<sub>2</sub> powder as the reagent in mild reaction conditions, up to 63 g of  $\beta$ -NaGdF<sub>4</sub>:Yb and Er@NaYF<sub>4</sub> nanoparticles of similar size and luminescent intensity comparing to their small-scale counterparts, could be obtained in one batch, which therefore shows the potential for large-scale preparation of other UCNPs.<sup>[52]</sup>

Thermal decomposition is generally considered as the typical and popular way to synthesize high-quality UCNPs, although there are still limitations to its industrial application. The synthesis process usually involves expensive and air-sensitive precursors and solvents, in addition to the need for high temperatures with the generation of toxic by-products.

## 2.2. Co-Precipitation

The co-precipitation method is another common operation to synthesize high-quality UCNPs. Compared with the traditional thermal decomposition method, high-temperature co-precipitation provides a better solution from an industrial perspective offering more environmentally friendly reagents containing inorganic rare earth salts. The method was first used by Zhang et al. (2008) by forming small NaYF<sub>4</sub> crystal nuclei at room



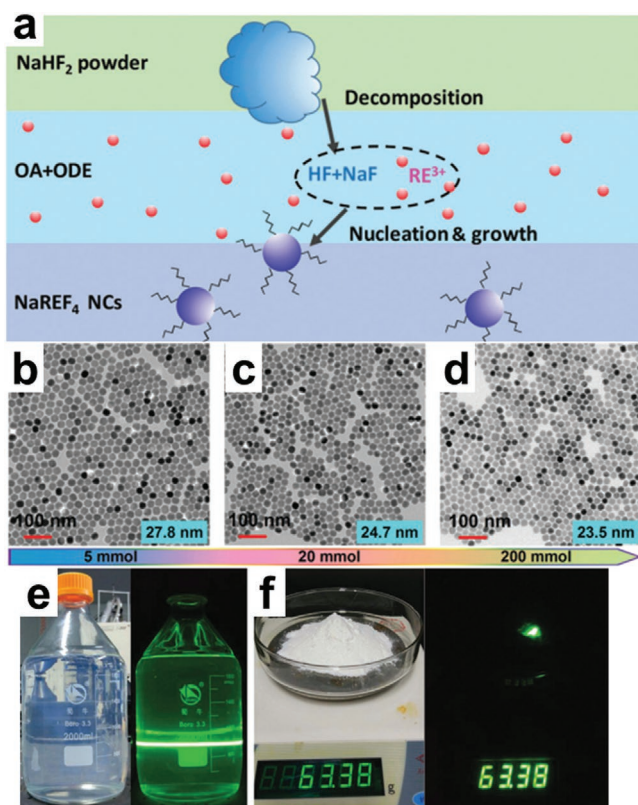


**Figure 2.** a) Schematic diagram of the proposed SLTD method for the synthesis of NaREF<sub>4</sub> UCNPs. TEM images for the synthesis of  $\beta$ -NaGdF<sub>4</sub>:Yb, Er UCNPs in different amounts: b) 5 mmol, c) 20 mmol, and d) 200 mmol. e) Photographs of the obtained  $\beta$ -NaGdF<sub>4</sub>:Yb,Er@NaYF<sub>4</sub> NCs dispersed in 2 L cyclohexane (left) and upon excitation at 980 nm (right). f) Photographs of the obtained NCs weight under room light (left) and upon excitation at 980 nm (right). Reproduced with permission.<sup>[52]</sup> Copyright 2018, The Royal Society of Chemistry.

temperature.<sup>[53]</sup> The temperature was then increased to promote further Ostwald ripening with an aim to reduce the toxic reagents and the involvement of by-products. In order to investigate the detailed reaction process, Suter et al. (2014)<sup>[54]</sup> used instant NIR-to-visible upconversion emission signals during the

heating-up process. They then divided the reaction time into four stages according to the real-time spectroscopic monitoring results as shown in **Figure 3**. During the first and second stages,  $\alpha$ -phase particles start to form and then stabilize. Later in stage three, the  $\alpha$ -phase begins to transform into the  $\beta$ -phase, followed by ripening and finally particle growth in stage four.<sup>[59]</sup> More recently, the high-temperature co-precipitation method has been used in the synthesis of a wider range of UCNPs: including NaYF<sub>4</sub>,<sup>[60]</sup> NaLuF<sub>4</sub>,<sup>[61]</sup> LiYF<sub>4</sub>,<sup>[62]</sup> KLu<sub>2</sub>F<sub>7</sub>,<sup>[63]</sup> NaGdF<sub>4</sub>,<sup>[64]</sup> NaYbF<sub>4</sub>,<sup>[65]</sup> LiYbF<sub>4</sub>,<sup>[66]</sup> and KSc<sub>2</sub>F<sub>7</sub>.<sup>[67]</sup> With proper optimization of the conditions, uniform 4 nm NaREF<sub>4</sub> UCNPs with enhanced upconversion luminescence could be achieved.<sup>[68]</sup>

It should be noted that temperature plays an important role in the nucleation and ripening stage, which may be affected when scaled up. This is because the increase of reaction volume amplifies the effect of inefficient mass and heat transfer, possibly resulting in an uneven temperature distribution inside the reaction system. This may cause a broad size distribution and the appearance of undesirable shapes.<sup>[29]</sup> To address this issue, Wihelm et al. (2015) designed an instant upconversion luminescence feedback device (**Figure 4**) to make sure the growth stage of  $\beta$ -NaYF<sub>4</sub> was controlled under 200 °C. The output provided was found to be more than 2 g of OA coated  $\beta$ -UCNPs with uniform phase and morphology in one batch, offering a potential approach for future production scale up.<sup>[69]</sup>

Another option to eliminate the ineffective heating process in the synthesis route is to bring down the reaction temperature. Recently the co-precipitation method has been used to synthesize upconversion nanoparticles under low temperatures or even room temperature conditions. Shao et al. (2014) synthesized monodisperse YF<sub>3</sub>:RE<sup>3+</sup> (RE = Eu, Ce, Tb, etc.) under low temperatures ( $\leq 0$  °C).<sup>[70]</sup> The low temperature led to the decline in the particles growth rate and diffusion coefficient, which could greatly sharpen the size distribution and achieve the synthesis of highly uniform and monodisperse UCNPs. Lei et al. (2017) chose NaBiF<sub>4</sub> as the upconversion host matrix, synthesizing NaBiF<sub>4</sub>:Yb<sup>3+</sup>/Er<sup>3+</sup> under room temperature. The replacement of commonly used rare earth elements such as yttrium with bismuth species significantly mitigated the reaction conditions while not compromising on the upconversion luminescence.<sup>[71]</sup>

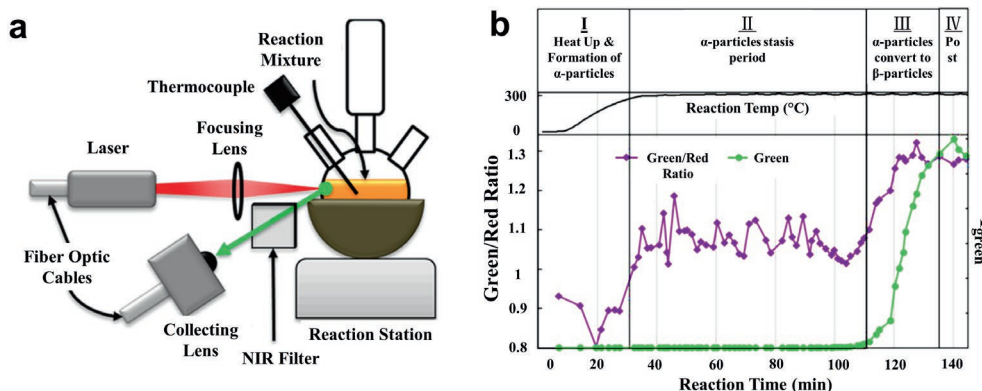


**Figure 3.** a) Schematic diagram of the experimental set up for real-time monitoring of UCNPs synthesis. Reproduced with permission.<sup>[54]</sup> Copyright 2014, American Chemical Society. b) Schematic illustration of the spectroscopic signal of green and red upconversion luminescent corresponding to the four stages mentioned in the synthesis of NaYF<sub>4</sub> nanoparticles. Reproduced with permission.<sup>[59]</sup> Copyright 2016, American Chemical Society.

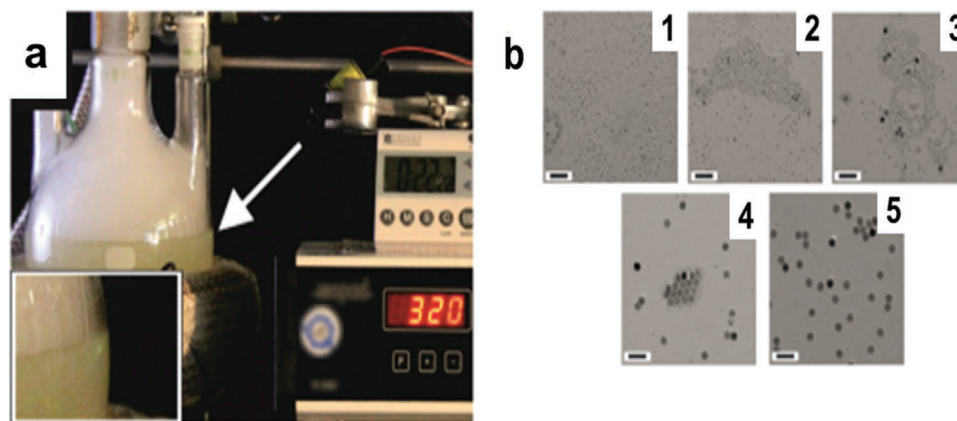


**Figure 4.** a) Images of experimental setup for large-scale synthesizing of  $\beta$ - $\text{NaYF}_4\text{:Yb}^{3+}$ ,  $\text{Er}^{3+}$  nanoparticles. Detectable green upconversion luminescence after 22 min was shown in the inset. b) TEM images of the obtained  $\beta$ - $\text{NaYF}_4\text{:Yb}^{3+}$ ,  $\text{Er}^{3+}$  nanoparticles after different reaction times: 10 min (1), 15 min (2), 22 min (3), 27 min (4), and 60 min (5). Reproduced with permission.<sup>[69]</sup> Copyright 2015, The Royal Society of Chemistry.

### 2.3. Hydrothermal

Hydrothermal/solvothermal is another common approach to synthesize UCNPs with desirable and controllable shapes and morphologies. Generally, it involves specific temperatures and pressures where the solvents inside the reaction vessels reach their critical or supercritical state. Altering the solubility and viscosity inside the reaction system benefits the solvent convection and solute diffusion. Usually the UCNPs hydrothermal synthesis approach does not need to have an inert atmosphere or high temperatures, making it a simpler operation. A typical hydrothermal process is demonstrated by Li et al. (2005), also known as the liquid–solid solution (LSS) process.<sup>[72]</sup> The process involves the nucleation of nanoparticles, which occurs due to the ion exchange and phase transfer across the interface of sodium linoleate (solid) and water–ethanol (solution). The linoleic acid in the liquid phase (liquid) then absorbs on the nanoparticles, leading to a spontaneous phase-separation process and thereby collecting them. Currently, the hydrothermal approach has been successful in the synthesis of  $\text{Gd}_2\text{O}_3$ ,<sup>[73]</sup>  $\text{Y}_2\text{O}_3$ ,<sup>[74]</sup>  $\text{ZnMoO}_4$ ,<sup>[75]</sup>  $\text{LaVO}_4$ ,<sup>[76]</sup>  $\text{NaLuF}_4$ ,<sup>[77]</sup> and  $\text{Sr}_2\text{SF}_7$ .<sup>[78]</sup>

During the process, the linoleic acid, functioning as the capping ligands, takes on an important role as the nucleation and growth rates can be easily regulated by adjusting the type and concentration of selected ligands.<sup>[79]</sup> Many different ligands including sodium citrate<sup>[80]</sup> ( $\text{Na}_3\text{Cit}$ ), sodium linoleate,<sup>[81]</sup> oleic acid<sup>[82]</sup> (OA), and disodium ethylenediaminetetraacetic acid<sup>[76]</sup> ( $\text{Na}_2\text{EDTA}$ ) have been used in accelerating the rate of particle formation. In particular, Liu et al. (2016) specialized the role of OA in the formation of  $\text{NaYF}_4$  and  $\text{NaGdF}_4$  particles.<sup>[83]</sup> OA, and its dissociated form  $\text{OA}^-$ , had different binding preferences due to the different facets present. Thus, by moderating the ratio of  $\text{OA}^-/\text{OA}$ , particle growth direction could be well determined, and particles with various longitudinal lengths and aspect ratios, ranging from about 0.2 to over 0.9, could be obtained (Figure 5). Also, apart from the ligands, other experimental factors including reaction temperature and time, volume ratios of ethanol to water, alcohol type, and subsequent annealing could also affect the morphology of the particles.<sup>[84–86]</sup>

Due to the involvement of capping ligands in the synthesis route, which are usually involved in UCNPs synthesis via the hydrothermal method, a hydrophobic surface will usually be present. This does not meet biological need. Therefore, a subsequent modification is required to convert the hydrophobic surface into a hydrophilic one. On the other hand, a one-pot synthetic hydrothermal route to obtain water-soluble UCNPs has been developed as a simple user-friendly alternative way. This approach employs pre-prepared rare earth stearates as precursors and capping ligands. They not only serve as morphology regulators in the hydrothermal process, but also introduce functional groups, including carboxyl groups, onto the surface of UCNPs,<sup>[87,88]</sup> turning the surface into hydrophilic. Recently, Han et al. (2016) proposed a novel way to synthesize UCNPs capped with both carboxyl and amino groups at the same time. Using amino acid as the stabilizer and capping ligands, the introduced carboxyl and amino groups could conjugate with different biomolecules simultaneously, allowing them to be better used in biological applications.<sup>[89]</sup>

Apart from the use of surfactants, impurity doping into UCNPs has been found to be another convenient way to alter the microscopic and macroscopic structures of nanoparticles. Wang et al. (2010) found that doping  $\text{Gd}^{3+}$  into the host lattice of  $\text{NaYF}_4$  during the hydrothermal process could greatly enhance the phase transfer from cubic ( $\alpha$ ) to hexagonal ( $\beta$ ), and a rod-like morphology could also be favored.<sup>[90]</sup> Following this, the result was extended to other rare earth ions with large ionic radii such as  $\text{La}^{3+}$  and  $\text{Ce}^{3+}$ .<sup>[91]</sup> At the same time, the impurity doping could break down the crystal field symmetry of lanthanide ions to some extent. Thus, by controlling the impurity dopant concentration, an enhanced upconversion luminescence intensity at a certain environment could be observed.<sup>[92,93]</sup>

The pivotal roles of surfactants and dopant concentrations on the particle characteristics in the hydrothermal process highlights the requirement for uniform concentration distribution inside the reaction system. However, the mixing mechanism occurring inside the reactor is inevitably affected during the scaling of the hydrothermal preparation process. Although there has been a report on the production of over 0.5 g of  $\text{NaYF}_4$  microplates via a facile template-free hydrothermal process in

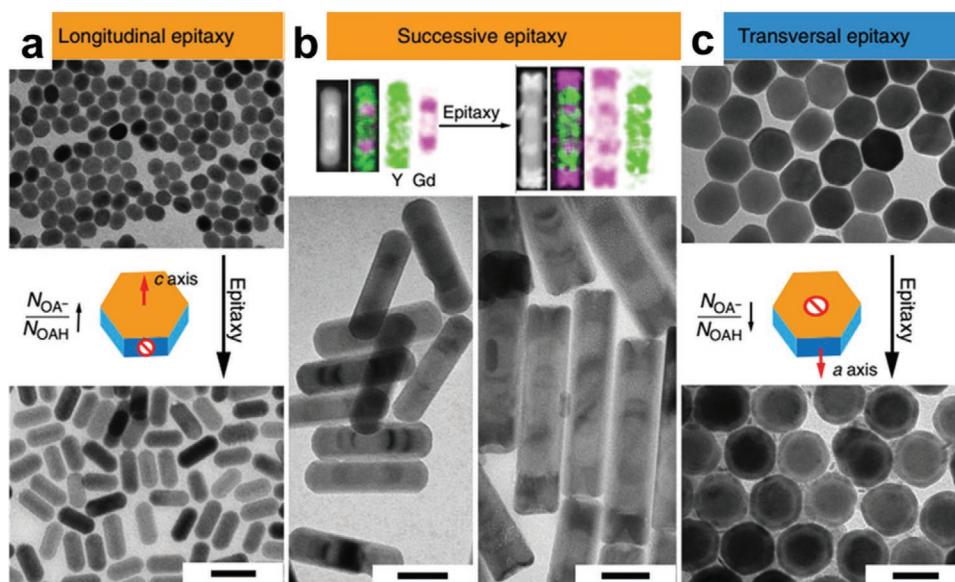


**Figure 5.** a) Longitudinal epitaxy growth of  $\text{NaYF}_4$  with  $\text{NaYF}_4$  core and homogeneous  $\text{NaYF}_4$  nanoparticles at  $310^\circ\text{C}$  for 1 h at NaOH to OA molar ratio of 1:19. b) Longitudinal epitaxy growth of periodical shells of  $\text{NaGdF}_4$ - $\text{NaYF}_4$  and  $\text{NaGdF}_4$ - $\text{NaYF}_4$ - $\text{NaGdF}_4$  onto core  $\text{NaYF}_4$  to form into five-section and seven-section “bamboo-shaped”  $\text{NaYF}_4$ / $\text{NaGdF}_4$  nanorods. Reaction was set at  $310^\circ\text{C}$  with 0.5 mmol NaOH and 0.4 mmol KOH and 9.5 mmol OA involved. c) Transversal epitaxy growth of  $\text{NaGdF}_4$  with  $\text{NaYF}_4$  core and homogeneous  $\text{NaYF}_4$ / $\text{NaGdF}_4$  nanoparticles at  $290^\circ\text{C}$  for 3 h at NaOH to OA molar ratio of 3:380 (Scale bar, 50 nm). Reproduced with permission.<sup>[83]</sup> Copyright 2016, Nature Publishing Group.

one batch with optimized experimental parameters,<sup>[94]</sup> it should be noted that the future industrialization of the hydrothermal preparation route is still hampered by the long reaction time, ranging from 12 to 24 h or even longer. Apart from that, high pressures, large solvent volumes as well as poor reproducibility are also key issues that need to be addressed.

## 2.4. Ion Exchange

Ion exchange, based on the hydrothermal technique provides another alternative synthesis route for UCNPs. Compared with the traditional synthesis approaches mentioned above, ion-exchange synthesis provides a facile way to control size and morphology of UCNPs while eliminating the involvement of toxic organic solvent.

Generally, ion exchange is used in nanoparticle surface ligand modification of UCNPs for a hydrophilic surface<sup>[95,96]</sup> and in the epitaxial shell growth process.<sup>[97]</sup> However, recently this method was found to be used in the synthesis of UCNPs core particles such as  $\text{NaYF}_4$ ,  $\text{NaGdF}_4$ ,  $\text{NaErF}_4$ , and  $\text{Na}_3\text{ZrF}_7$ .<sup>[98–101]</sup> Usually the synthesis route involves two or three stages, as shown in **Figure 6**. In the first stage, a precursor with a structure that is closely matched with the desired crystal and has both a similar sub-lattice symmetry and atomic stacking is synthesized.<sup>[99]</sup> After that, the pre-prepared precursor is mixed with an aqueous mixture for further reaction, which includes hydrothermal or thermal decomposition reaction to prepare the desired nanocrystals. By varying the precursor type and shape, easy control of the morphology and shape of the UCNPs is allowed.<sup>[102]</sup> Recently, a novel approach, the topotactic transformation strategy, has been developed based on the ion-exchange method. This approach only requires partial

structural matching between the precursors and obtained nanoparticles. For example, Shao et al. (2016)<sup>[103]</sup> synthesized monodisperse  $\beta$ - $\text{NaYF}_4$  by using  $\text{NaY}(\text{CO}_3)\text{F}_2$  as precursors due to the similarity of the atomic arrangement along the [001] direction between  $\beta$ - $\text{NaYF}_4$  and  $\text{NaY}(\text{CO}_3)\text{F}_2$ .<sup>[104]</sup> Using the same process, they developed the in situ synthesis of YOF microcrystals by using  $\text{Y}_4\text{O}(\text{OH})_9\text{NO}_3$  particles based on the topotactic similar structures.<sup>[105]</sup>

There are some other synthesis approaches that have been used for the synthesis of UCNPs including the sol–gel<sup>[106,107]</sup> and electrospinning methods.<sup>[108,109]</sup> However, the potential of mass production and precise control over these methods are hindered by large solvent volumes, complex multistep operations, and poor reproducibility, thus limiting the promotion of future commercial applications.

## 3. Continuous Reactors

To achieve a high performance and efficient mass production of nanoparticles, flow processes and reactors have emerged as the main focus in which continuous operation provides better heat and mass transfer, reducing the cost and waste throughout the process as well as delivering higher yields.<sup>[110–112]</sup> To date, several continuous synthesis routes to obtain UCNPs have been classified and reported as follows.

### 3.1. Microfluidics

The microfluidic synthesis route was first discussed by deMello (2002)<sup>[113]</sup> aiming at the synthesis of a wide range of nanocrystals, including iron oxide nanoparticles<sup>[114]</sup> and semiconductor



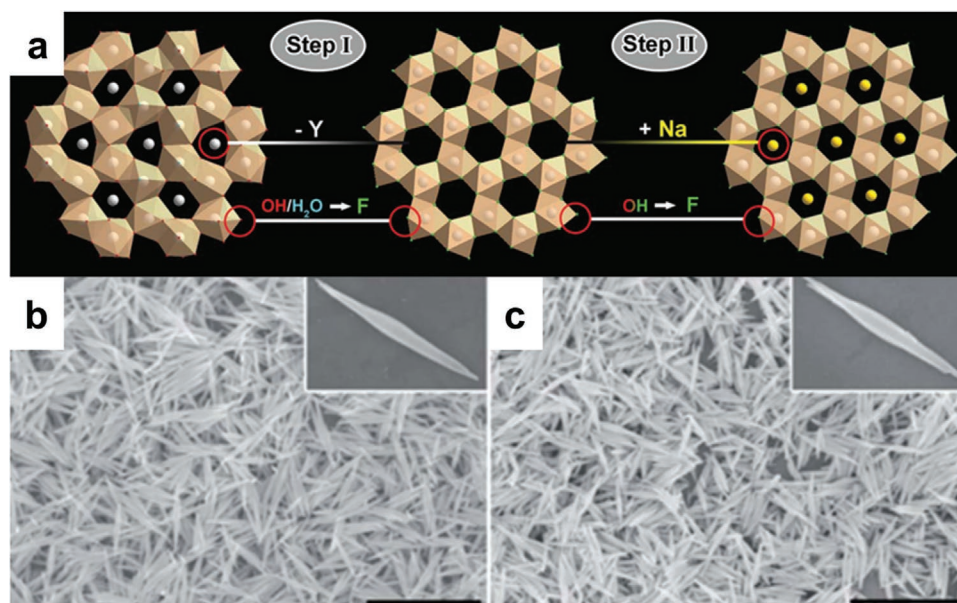


**Figure 6.** a) Schematic illustration of ion-exchange synthesis mechanism from  $\text{Y}(\text{OH})_{1.57}\text{F}_{1.43}$  precursors to  $\beta\text{-NaYF}_4$  product. b) SEM images of the as-prepared  $\text{Y}(\text{OH})_{1.57}\text{F}_{1.43}$  precursors. c) SEM images of the synthesized  $\beta\text{-NaYF}_4$  product. Reproduced with permission.<sup>[99]</sup> Copyright 2015, The Royal Society of Chemistry.

quantum dots.<sup>[115]</sup> However, their application in the synthesis of UCNPs has been rarely reported. It was reported by Zhu et al. (2008) that upconverting  $\text{LaF}_3\text{:Ce, Tb}$  could be prepared in a capillary microfluidic reactor.<sup>[116]</sup> **Figure 7a.** The precursors were pumped into the reaction system at a consistent rate through syringes, then mixed and reacted in the heated microcapillary and finally collected in the microcapillary outlet. Despite the reaction being similar to the conventional reaction, the microcapillary provides rapid and efficient mixing, broadening the operating condition ranges for the synthesis reaction. Compared with samples collected at the outlet of the microcapillaries at 180 °C for 3 s or at the bottle of the oven at 100 °C for 30 min, the method which uses the sample to be collected at the outlet of the microcapillary under two different reaction temperatures initially 180 °C for 3 s then 100 °C for 30 s

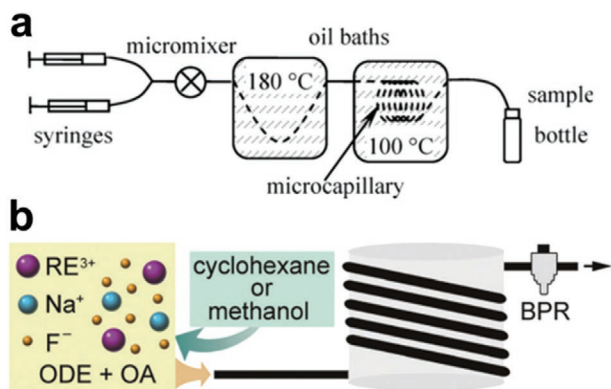


**Figure 7.** a) Microfluidic reactor for the synthesis of  $\text{LaF}_3\text{:Ce, Tb}$  nanoparticles. Adapted with permission.<sup>[116]</sup> Copyright 2008, The Royal Society of Chemistry. b) Illustration of flow reactor for the synthesis of  $\text{NaGdF}_4\text{:Yb/Er}$  upconversion nanocrystals. Reproduced with permission.<sup>[104]</sup> Copyright 2016, The Royal Society of Chemistry.

in two separate oil baths, Figure 7a, gave more accurate control over the two different reaction stages, higher temperature bath to burst nuclei and lower temperature to promote growth, resulting in a controllable crystallization process.<sup>[116]</sup> Following this, they replaced the traditional oil heating capillary reactor with a microwave irradiation capillary reactor. With the addition of microwave technique, a better micromixing was achieved by polarizing the solvent and reagent, resulting in a more homogeneous temperature diffusion. Through this way, size distribution was narrowed down and aggregation was reduced.<sup>[117]</sup>

Furthermore, Che et al. (2014) demonstrated to use microfluidic technologies for nanoparticles syntheses at the nucleation growth stages, to promote crystallization at a certain extent.<sup>[118]</sup> These findings were also attributed to the homogeneous mixing inside the reaction system, enabling accurate control of the reaction parameters. Similarly, Jiao et al. (2016) reported a novel  $\text{NaGdF}_4\text{:Yb/Er}$  nanocrystal synthesis route based on microfluidic technology. Experimental conditions for the tube reactor of 260 °C and 30 bar produced  $\text{NaGdF}_4\text{:Yb/Er}$  nanocrystals under 5 nm with a narrow size distribution.<sup>[104]</sup> Figure 7b. More importantly, with the involvement of a flow reactor in this process, a higher reaction pressure is present. Thus, by altering the solvents, using different boiling points, viscosities, and polarities, nanoparticles of different sizes could be achieved without sacrificing monodispersity. Continuous production could avoid the disadvantage of poor batch-to-batch reproducibility that arises from traditional batch production, the microfluidic route thus shows huge potential in future scalability for the synthesis of other UCNPs.

### 3.2. High Gravity

High-gravity technology, also known as HIGEE technology, is a common method for process intensification within particle



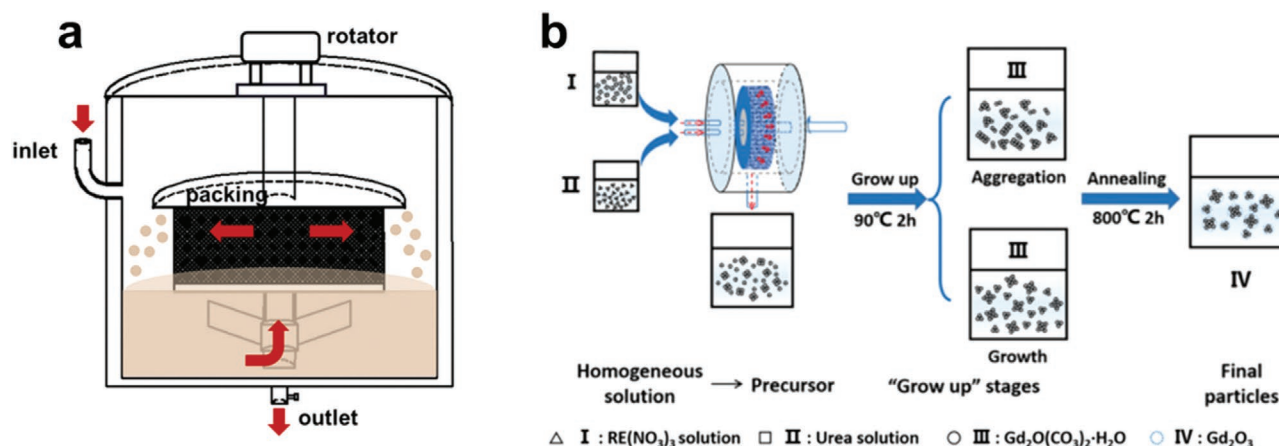


**Figure 8.** a) Schematic illustration of a typical RPB reactor for synthesizing nanoparticles. Adapted with permission.<sup>[134]</sup> Copyright 2019, American Chemical Society. b) Schematic diagram of a typical high-gravity preparation route for UCNPs. Reproduced with permission.<sup>[131]</sup> Copyright 2017, American Chemical Society.

synthesis. First reported by Ramshaw (1979),<sup>[119,120]</sup> it has been widely used in the synthesis of different nanoparticles, such as drug particles,<sup>[121]</sup> nanophosphors,<sup>[122]</sup> photocatalysts,<sup>[123]</sup> and semiconductor quantum dots.<sup>[124,125]</sup> The high-gravity method normally is fulfilled by a rotating packed bed reactor (RPB) which intensifies the reaction process via generating a high-gravity environment.<sup>[125]</sup> A typical structure of an RPB is illustrated in **Figure 8**, which consists of a rotator, packing reactor, pumps, valves, and outlets. The liquid containing precursors and solvents are introduced to the reactor through pumps, spraying to the inside edge of rotator via a slotted pipe distributor. It enters the bed flowing in the radial direction under centrifugal force, finally being collected in the outlets.<sup>[126]</sup> During the process, the liquid flow is dispersed consistently by the distributor, splitting into nanodroplets, threads, and thin films in the packing, then contacting each other for reaction. Thus, micromixing time is greatly reduced and micromixing efficiency is improved, resulting in a homogeneous reaction system.<sup>[127,128]</sup> Due to its unique characteristics, RPB technology is viewed as an efficient way to scale up nanoparticle production while narrowing down the size distribution.<sup>[129,130]</sup> Recently, our group employed the RPB reactor in the  $\text{Gd}_2\text{O}_3$  synthesis route to obtain monodisperse  $\text{Gd}_2\text{O}_3\text{:Yb}^{3+}/\text{Er}^{3+}$  nanoparticles with good optical performance. Compared with the stirred tank reactor (STR), UCNPs prepared by HIGEE technology produced an average particle size of 100 nm, compared with 360 nm in STR, which could then be well dispersed in transparent waterborne polyurethane (PU) films after modification.<sup>[131]</sup> Later, we employed this same approach in the synthesis of upconversion  $\text{NaYF}_4$  nanocrystals. With involving the RPB reactor, a decrease in microrod size and diameter distribution was achieved, which showed a good potential in anti-counterfeiting applications.<sup>[132]</sup>

At the same time, the mass transfer and liquid mixing efficiency in RPB reactors are enhanced by several orders of magnitude, due to its unique structures.<sup>[120,133]</sup> This promotes the homogeneous distribution of reagent concentrations, supersaturation diffusion, and temperature gradient

inside the reactor even with a high liquid holdup. RPB reactors overcome the limitations of conventional batch reactors and provide a promising way for future scale up. Based on this, we reported a scalable synthesis route for  $\beta\text{-NaYF}_4$  in an RPB reactor. More than 1 g of  $\text{NaYF}_4\text{:Gd}^{3+}/\text{Yb}^{3+}/\text{Er}^{3+}$  nanoparticles with uniform morphology and phase could be obtained at a time, with similar particles morphology and luminescent properties to the small-scale synthesis.<sup>[134]</sup> The result further proves the great potential of RPB technology for mass production of UCNPs.

### 3.3. Mechanochemical Preparation

The UCNPs synthesis approaches mentioned above require the involvement of organic or inorganic solvents, which serve as the reaction environment or capping ligands. However, these have greater potential in promoting negative environmental effects caused by toxic organic solvents. The solid-solution-based mechanochemical preparation method, which eliminates the use of liquid-based reagents, could overcome these limitations. For example, the ball milling synthesis method—a typical mechanochemical preparation method has been widely applied to several nanoparticles synthesis systems, such as  $\text{LiFePO}_4\text{-C}$  composite<sup>[135]</sup> and  $\text{ZnO}$  nanowires.<sup>[136]</sup> A typical ball milling setup is illustrated in **Figure 9**. Pre-ground and dried precursors are injected into a zirconia jar with two zirconia balls inside the jar. The jar is sealed for the balling milling process and nitrogen gas environment is provided. Riesen et al. (2015) used this method for the preparation of  $\text{NaYF}_4$ .<sup>[137]</sup> Compared with the conventional methods, the reaction can be conducted at room temperature and no subsequent annealing processes were needed. Till now, the ball milling method has been successfully applied to other luminescent materials including  $\text{BaFCl}$ ,<sup>[138]</sup>  $\text{SrFCl}$ ,<sup>[139]</sup> and  $\text{Y}_3\text{Al}_5\text{O}_{12}$ ,<sup>[140]</sup> all of which showed excellent luminescent intensity. Without involving liquid solvent, mechanochemical preparation method offer a green, low-cost, and highly scalable synthesis route of UCNPs.

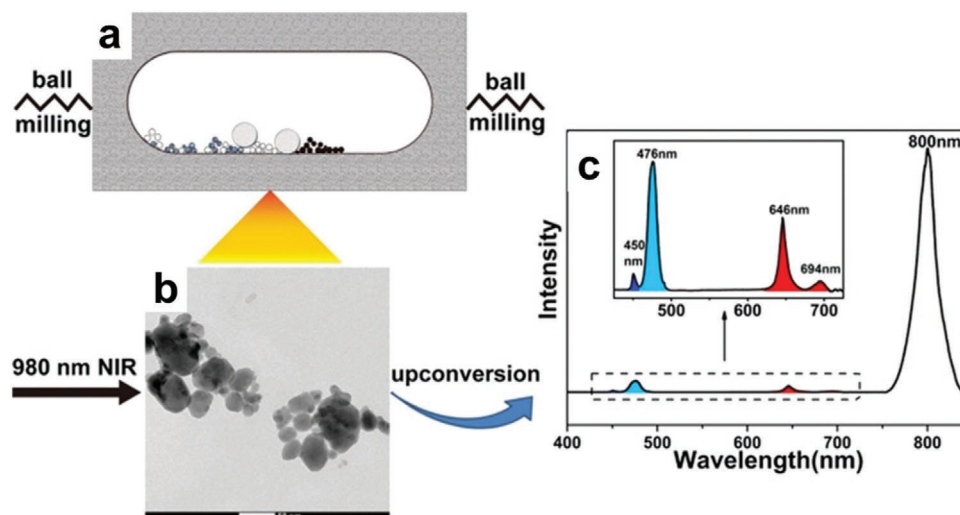


**Figure 9.** Schematic illustration of mechanochemical preparation process including a) diagram of mechanochemical chemical reactor, b) TEM images of NaYF<sub>4</sub>:Yb, Tm UCNPs, and c) upconversion luminescence spectra upon excitation at 980 nm. Reproduced with permission.<sup>[137]</sup> Copyright 2015, Elsevier.

## 4. Conclusion

Compared with the concurrent researches that has been devoted from synthetic methods to the applications of UCNPs, less attention have been paid to the limitations of existing scaling-up techniques for mass production of high-quality UCNPs. In this article, we provide a glance view of recent advances in UCNPs synthesis approaches, with particular interest on the potential for future scale-up production. Generally, considerable progresses have been made to simplify synthesis operation by mitigating the reaction conditions toward a substantial greener synthesis. Nevertheless, the challenge to create efficient heat and mass transfer during the synthesis remains to be resolved, which potentially affects the overall nanoparticle morphology and optical performances. These concerns could be fixed through optimizing the traditional batch-to-batch synthesis route, as well as using flow synthesis systems. The continuous preparation method seems to be the winner of all candidates, since it will lead to benefits including an enhanced micromixing function with increased precision control on experimental parameters and potential cost and waste reduction.

Despite these developments, we conclude that the following issues and actions remain on the engineering and industrial production areas, which need to be coped appropriately with the existing problems and to drive the effective industrial production of UCNPs in future:

1. It should be noticed that in the commonly reported synthesis route core parameters such as throughput and process yield are still missing. Small reaction size and limited product quantity are disadvantages when trying to meet industrial demands.
2. A better understanding on the mixing mechanism from the scaling-up points of view is highly demanded, which require proper simulation tools such as CFD models.
3. As luminescence properties of UCNPs are highly dependent on their shapes, sizes, and phases, the correlation mechanisms between them need be developed in an advanced level for the future scale up and mass production of UCNPs.

## Acknowledgements

The authors are grateful for financial support from the National Natural Science Foundation of China (21808009) and the Beijing Natural Science Foundation (2182051). S.W. acknowledges the financial support from the City University of Hong Kong (startup grant). The work was supported by the Engineering and Physical Sciences Research Council (EPSRC) grant-EP/N007921 and Royal Society Kan Tong Po International Fellowship 2019—KTP\R1\191012.

## Conflict of Interest

The authors declare no conflict of interest.

## Keywords

process intensification, scale up, synthesis, upconversion nanophosphors

Received: April 29, 2020

Revised: June 14, 2020

Published online: August 16, 2020

- [1] U. Resch-Genger, M. Grabolle, S. Cavaliere-Jaricot, R. Nitschke, T. Nann, *Nat. Methods* **2008**, 5, 763.
- [2] X. Michalet, F. F. Pinaud, L. A. Bentolila, J. M. Tsay, S. Doose, J. J. Li, G. Sundaresan, A. M. Wu, S. S. Gambhir, S. Weiss, *Science* **2005**, 307, 538.
- [3] H. T. Sun, Y. Sakka, *Sci Technol Adv. Mat.* **2014**, 15, 14205.
- [4] X. Z. Lim, *Nature* **2016**, 531, 26.
- [5] S. Van Loy, K. Binnemans, T. Van Gerven, *Engineering* **2018**, 4, 398.
- [6] W. Zheng, P. Huang, D. T. Tu, E. Ma, H. M. Zhu, X. Y. Chen, *Chem. Soc. Rev.* **2015**, 44, 1379.
- [7] F. Wang, X. G. Liu, *Chem. Soc. Rev.* **2009**, 38, 976.
- [8] N. Bloembergen, *Phys. Rev. Lett.* **1959**, 2, 84.
- [9] J. F. Porter Jr., *Phys. Rev. Lett.* **1961**, 7, 414.
- [10] F. Auzel, *Chem. Rev.* **2004**, 104, 139.
- [11] C. C. Duan, L. E. Liang, L. Li, R. Zhang, Z. P. Xu, *J. Mater. Chem. B* **2018**, 6, 192.

- [12] S. Chen, A. Z. Weitemier, X. Zeng, L. M. He, X. Y. Wang, Y. Q. Tao, A. J. Y. Huang, Y. Hashimoto, M. Kano, H. Iwasaki, L. K. Parajuli, S. Okabe, D. B. L. Teh, A. H. All, I. Tsutsui-Kimura, K. F. Tanaka, X. G. Liu, T. J. McHugh, *Science* **2018**, 359, 679.
- [13] D. Wang, L. Zhu, Y. Pu, J. X. Wang, J. F. Chen, L. M. Dai, *Nanoscale* **2017**, 9, 11214.
- [14] N. Moller, T. Hellwig, L. Stricker, S. Engel, C. Fallnich, B. J. Ravoo, *Chem. Commun.* **2017**, 53, 240.
- [15] H. J. Chang, J. Xie, B. Z. Zhao, B. T. Liu, S. L. Xu, N. Ren, X. J. Xie, L. Huang, W. Huang, *Nanomaterials* **2015**, 5, 1.
- [16] M. Nyk, R. Kumar, T. Y. Ohulchanskyy, E. J. Bergey, P. N. Prasad, *Nano. Lett.* **2008**, 8, 3834.
- [17] Z. Y. Hou, C. X. Li, P. A. Ma, Z. Y. Cheng, X. J. Li, X. Zhang, Y. L. Dai, D. M. Yang, H. Z. Lian, J. Lin, *Adv. Funct. Mater.* **2012**, 22, 2713.
- [18] L. L. Liang, Y. M. Liu, C. H. Bu, K. M. Guo, W. W. Sun, N. Huang, T. Peng, B. Sebo, M. M. Pan, W. Liu, S. S. Guo, X. Z. Zhao, *Adv. Mater.* **2013**, 25, 2174.
- [19] R. K. Das, J. P. Kar, S. Mohapatra, *Ind. Eng. Chem. Res.* **2016**, 55, 5902.
- [20] G. Chen, H. Qiu, P. N. Prasad, X. Che, *Chem. Rev.* **2014**, 114, 5161.
- [21] R. B. Anderson, S. J. Smith, P. S. May, M. T. Berry, *J. Phys. Chem. Lett.* **2014**, 5, 36.
- [22] M. T. Berry, P. S. May, *J. Phys. Chem. A* **2015**, 119, 9805.
- [23] C. L. Chen, C. G. Li, Z. Shi, *Adv. Sci.* **2016**, 3, 1600029.
- [24] M. Kaiser, C. Wurth, M. Kraft, I. Hyppanen, T. Soukka, U. Resch-Genger, *Nanoscale* **2017**, 9, 10051.
- [25] V. Muhr, C. Wurth, M. Kraft, M. Buchner, A. J. Baumner, U. Resch-Genger, T. Hirsch, *Anal. Chem.* **2017**, 89, 4868.
- [26] D. Yuan, M. C. Tan, R. E. Riman, G. M. Chow, *J. Phys. Chem. C* **2013**, 117, 13297.
- [27] P. L. Saldanha, V. Lesnyak, L. Manna, *Nano Today* **2017**, 12, 46.
- [28] L. Gonzalez-Moragas, S. M. Yu, N. Murillo-Cremaes, A. Laromaine, A. Roig, *Chem. Eng. J.* **2015**, 281, 87.
- [29] A. Klinkova, E. M. Larin, E. Prince, E. H. Sargent, E. Kumacheva, *Chem. Mater.* **2016**, 28, 3196.
- [30] A. J. Grohn, S. E. Pratsinis, A. Sanchez-Ferrer, R. Mezzenga, K. Wegner, *Ind. Eng. Chem. Res.* **2014**, 53, 10734.
- [31] Y. Li, G. F. Wang, K. Pan, N. Y. Fan, S. Liu, L. Feng, *RSC Adv.* **2013**, 3, 1683.
- [32] T. Rinkel, J. Nordmann, A. N. Raj, M. Haase, *Nanoscale* **2014**, 6, 14523.
- [33] Q. Zhao, B. Q. Shao, W. Lu, W. Z. Lv, M. M. Jiao, L. F. Zhao, H. P. You, *Dalton Trans.* **2015**, 44, 3745.
- [34] J. C. Boyer, L. A. Cuccia, J. A. Capobianco, *Nano Lett.* **2007**, 7, 847.
- [35] Y. W. Zhang, X. Sun, R. Si, L. P. You, C. H. Yan, *J. Am. Chem. Soc.* **2005**, 127, 3260.
- [36] J. C. Boyer, F. Vetrone, L. A. Cuccia, J. A. Capobianco, *J. Am. Chem. Soc.* **2006**, 128, 7444.
- [37] K. Nigoghossian, S. Ouellet, J. Plain, Y. Messaddeq, D. Boudreau, S. J. L. Ribeiro, *J. Mater. Chem. B* **2017**, 5, 7109.
- [38] I. K. M. M. Sahib, T. Asahi, D. Thangaraju, S. Kyohei, S. Yosuke, I. Wataru, K. Yoshimasa, H. Yasuhiro, *Part. Part. Syst. Charact.* **2018**, 35, 1800227.
- [39] Y. H. Yang, D. T. Tu, W. Zheng, Y. S. Liu, P. Huang, E. Ma, R. F. Li, X. Y. Chen, *Nanoscale* **2014**, 6, 11098.
- [40] H. Q. Wang, D. T. Tu, J. Xu, X. Y. Shang, P. Hu, R. F. Li, W. Zheng, Z. Chen, X. Y. Chen, *J. Mater. Chem. B* **2017**, 5, 4827.
- [41] H. X. Mai, Y. W. Zhang, L. D. Sun, C. H. Yan, *J. Phys. Chem. C* **2007**, 111, 13730.
- [42] B. Voss, M. Haase, *ACS Nano* **2013**, 7, 11242.
- [43] H. Na, K. Woo, K. Lim, H. S. Jang, *Nanoscale* **2013**, 5, 4242.
- [44] Y. Liu, Y. Lu, X. Yang, X. Zheng, S. Wen, F. Wang, X. Vidal, J. Zhao, D. Liu, Z. Zhou, C. Ma, J. Zhou, P. James A, P. Xi, D. Jin, *Nature* **2017**, 543, 229.
- [45] X. Zhai, Y. Wang, X. Liu, S. Liu, P. Lei, S. Yao, S. Song, L. Zhou, J. Feng, H. Zhang, *ChemPhotoChem* **2017**, 1, 369.
- [46] M. Casamonti, L. Risaliti, G. Vanti, V. Piazzini, M. C. Bergonzi, A. R. Bilia, *Engineering* **2019**, 5, 69.
- [47] B. A. Kairdolf, A. M. Smith, T. H. Stokes, M. D. Wang, A. N. Young, S. Nie, *Rev. Anal. Chem.* **2013**, 6, 143.
- [48] H. S. Choi, W. Liu, P. Misra, E. Tanaka, J. P. Zimmer, B. I. Ipe, G. M. Bawendi, J. V. Frangioni, *Nat. Biotechnol.* **2007**, 25, 1165.
- [49] C. Y. Cheng, Y. S. Xu, S. T. Liu, Y. Y. Liu, X. Wang, J. X. Wang, G. J. H. De, *J. Mater. Chem. C* **2019**, 7, 8898.
- [50] T. Rinkel, A. N. Raj, S. Duhnen, M. Haase, *Angew. Chem. Int. Ed.* **2016**, 55, 1164.
- [51] X. Y. Zhang, Z. Guo, X. Zhang, L. J. Gong, X. H. Dong, Y. Y. Fu, Q. Wang, Z. J. Gu, *Sci. Rep.* **2019**, 9, 5212.
- [52] W. W. You, D. T. Tu, W. Zheng, X. Y. Shang, X. R. Song, S. Y. Zhou, Y. Liu, R. F. Li, X. Y. Chen, *Nanoscale* **2018**, 10, 11477.
- [53] Z. Q. Li, Y. Zhang, S. Jiang, *Adv. Mater.* **2008**, 20, 4765.
- [54] J. D. Suter, N. J. Pekas, M. T. Berry, P. S. May, *J. Phys. Chem. C* **2014**, 118, 13238.
- [55] R. Shi, X. Ling, X. Li, L. Zhang, M. Lu, X. Xie, L. Huang, W. Huang, *Nanoscale* **2017**, 9, 13739.
- [56] A. N. Raj, T. Rinkel, M. Haase, *Chem. Mater.* **2014**, 26, 5689.
- [57] A. D. Ostrowski, E. M. Chan, D. J. Gargas, E. M. Katz, G. Han, P. J. Schuck, J. D. Milliron, B. E. Cohen, *ACS Nano* **2012**, 6, 2686.
- [58] N. J. Johnson, W. Oakden, G. J. Stanis, R. S. Prosser, F. C. Van Veggel, *Chem. Mater.* **2011**, 23, 3714.
- [59] P. B. May, J. D. Suter, P. S. May, M. T. Berry, *J. Phys. Chem. C* **2016**, 120, 9482.
- [60] M. Xu, X. M. Zou, Q. Q. Su, W. Yuan, C. Cao, Q. H. Wang, X. J. Zhu, W. Feng, F. Y. Li, *Nat. Commun.* **2018**, 9, 5212.
- [61] U. Stochaj, D. C. R. Burbano, D. R. Cooper, M. Kodiha, J. A. Capobianco, *Nanoscale* **2018**, 10, 14464.
- [62] X. Y. Jiang, C. Cao, W. Feng, F. Y. Li, *J. Mater. Chem. B* **2016**, 4, 87.
- [63] W. J. Bian, Y. Lin, T. Wang, X. Yu, J. B. Qiu, M. Zhou, H. M. Luo, S. F. Yu, X. H. Xu, *ACS Nano* **2018**, 12, 3623.
- [64] F. Wang, R. R. Deng, X. G. Liu, *Nat. Protoc.* **2014**, 9, 1634.
- [65] R. K. Shi, M. A. Ling, X. N. Li, L. Zhang, M. Lu, X. J. Xie, L. Huang, W. Huang, *Nanoscale* **2017**, 9, 13739.
- [66] Q. L. Zou, P. Huang, W. Zheng, W. W. You, R. F. Li, D. T. Tu, J. Xu, X. Y. Chen, *Nanoscale* **2017**, 9, 6521.
- [67] Y. B. Wang, T. Wei, X. W. Cheng, H. Ma, Y. Pan, J. Xie, H. Q. Su, X. J. Xie, L. Huang, W. Huang, *J. Mater. Chem. C* **2017**, 5, 3053.
- [68] E. Lu, J. Pichaandi, L. P. Arnett, L. Tong, M. A. Winnik, *J. Phys. Chem. C* **2017**, 121, 18178.
- [69] S. Wilhelm, M. Kaiser, C. Wurth, J. Heiland, C. Carrillo-Carrion, V. Muhr, O. S. Wolfbeis, W. J. Parak, U. Resch-Genger, T. Hirsch, *Nanoscale* **2015**, 7, 1403.
- [70] B. Q. Shao, Q. Zhao, Y. C. Jia, W. Z. Lv, M. M. Jiao, W. Lu, H. P. You, *J. Mater. Chem. C* **2014**, 2, 7666.
- [71] P. P. Lei, R. An, S. Yao, Q. S. Wang, L. L. Dong, X. Xu, K. M. Du, J. Feng, H. J. Zhang, *Adv. Mater.* **2017**, 29, 1700505.
- [72] X. Wang, J. Zhuang, Q. Peng, Y. D. Li, *Nature* **2005**, 437, 121.
- [73] Z. Liu, F. Pu, S. Huang, Q. H. Yuan, J. S. Ren, X. G. Qu, *Biomaterials* **2013**, 34, 1712.
- [74] L. B. Zong, P. F. Xu, Y. J. Ding, K. Zhao, Z. M. Wang, X. C. Yan, R. B. Yu, J. Chen, X. R. Xing, *Small* **2015**, 11, 2768.
- [75] H. N. Luitel, R. Chand, H. Hamajima, Y. R. Gaihre, T. Shingae, T. Yanagita, T. Watari, *J. Mater. Chem. B* **2016**, 4, 6192.
- [76] F. Zhang, G. Q. Li, W. F. Zhang, Y. L. Yan, *Inorg. Chem.* **2015**, 54, 7325.
- [77] H. Lin, D. K. Xu, A. M. Li, D. D. Teng, S. H. Yang, Y. L. Zhang, *J. Mater. Chem. C* **2015**, 3, 11754.
- [78] B. Zhao, D. Y. Shen, J. Yang, S. S. Hu, X. J. Zhou, J. F. Tang, *J. Mater. Chem. C* **2017**, 5, 3264.
- [79] W. F. Lai, A. L. Rogach, W. T. Wong, *Chem. Sci.* **2017**, 8, 7339.
- [80] C. X. Li, Z. W. Quan, J. Yang, P. P. Yang, J. Lin, *Inorg. Chem.* **2007**, 46, 6329.



- [81] L. Y. Wang, Y. D. Li, *Chem. Mater.* **2007**, 19, 727.
- [82] D. Wang, L. Zhu, J. F. Chen, L. M. Dai, *Angew. Chem. Int. Ed.* **2016**, 55, 10795.
- [83] D. M. Liu, X. X. Xu, Y. Du, X. Qin, Y. H. Zhang, C. S. Ma, S. H. Wen, W. Ren, E. M. Goldys, J. A. Piper, S. X. Dou, X. G. Liu, D. Y. Jin, *Nat. Commun.* **2016**, 7, 10254.
- [84] N. C. Dyck, F. C. J. M. van Veggel, G. P. Demopoulos, *ACS Appl. Mater. Interfaces* **2013**, 5, 11661.
- [85] G. Gao, C. L. Zhang, Z. J. Zhou, X. Zhang, J. B. Ma, C. Li, W. L. Jin, D. X. Cui, *Nanoscale* **2013**, 5, 351.
- [86] L. H. He, X. Zou, X. He, F. Y. Lei, N. Jiang, Q. J. Zheng, C. G. Xu, Y. F. Liu, D. M. Lin, *Cryst. Growth Des.* **2018**, 18, 808.
- [87] Z. Wang, X. H. Li, Y. C. Song, L. H. Li, W. Shi, H. M. Ma, *Anal. Chem.* **2015**, 87, 5816.
- [88] G. M. Han, H. Li, X. X. Huang, D. M. Kong, *Talanta* **2016**, 147, 207.
- [89] G. M. Han, H. X. Jiang, Y. F. Huo, D. M. Kong, *J. Mater. Chem. B* **2016**, 4, 3351.
- [90] F. Wang, Y. Han, C. S. Lim, Y. H. Lu, J. Wang, J. Xu, H. Y. Chen, C. Zhang, M. H. Hong, X. G. Liu, *Nature* **2010**, 463, 1061.
- [91] X. F. Yu, M. Li, M. Y. Xie, L. D. Chen, Y. Li, Q. Q. Wang, *Nano Res.* **2010**, 3, 51.
- [92] Y. Q. Wu, Y. Ji, J. Xu, J. J. Liu, Z. W. Lin, Y. L. Zhao, Y. Sun, L. Xu, K. J. Chen, *Acta Mater.* **2017**, 131, 373.
- [93] J. Tang, L. Chen, J. Li, Z. Wang, J. H. Zhang, L. G. Zhang, Y. S. Luo, X. J. Wang, *Nanoscale* **2015**, 7, 14752.
- [94] W. J. Yao, Q. Y. Tian, J. Liu, Z. H. Wu, S. Y. Cui, J. Ding, Z. G. Dai, W. Wu, *J. Mater. Chem. C* **2016**, 4, 6327.
- [95] W. Kong, T. Y. Sun, B. Chen, X. Chen, F. J. Ai, X. Y. Zhu, M. Y. Li, W. J. Zhang, G. Y. Zhu, F. Wang, *Inorg. Chem.* **2017**, 56, 872.
- [96] M. Guan, Z. G. Zhou, L. F. Mei, H. Zheng, W. Ren, L. Wang, Y. Du, D. Y. Jin, J. J. Zhou, *Chem. Commun.* **2018**, 54, 9587.
- [97] X. W. Liu, X. Y. Li, X. Qin, X. J. Xie, L. Huang, X. G. Liu, *Adv. Mater.* **2017**, 29, 1702315.
- [98] F. Zhang, D. Y. Zhao, *ACS Nano* **2009**, 3, 159.
- [99] B. Q. Shao, Q. Zhao, W. Z. Lv, M. M. Jiao, W. Lu, H. P. You, *J. Mater. Chem. C* **2015**, 3, 1091.
- [100] D. Q. Chen, Y. Liu, J. K. Chen, H. Huang, J. S. Zhong, Y. W. Zhu, *J. Mater. Chem. C* **2019**, 7, 1321.
- [101] B. Q. Shao, Q. Zhao, Y. C. Jia, W. Z. Lv, M. M. Jiao, W. Lu, H. P. You, *Chem. Commun.* **2014**, 50, 12706.
- [102] H. L. Wu, R. Sato, A. Yamaguchi, M. Kimura, M. Haruta, H. Kurata, T. Teranishi, *Science* **2016**, 351, 1306.
- [103] B. Q. Shao, Y. Feng, Y. Song, M. M. Jiao, W. Lu, H. P. You, *Inorg. Chem.* **2016**, 55, 1912.
- [104] M. X. Jiao, L. H. Jing, C. Y. Liu, Y. Hou, J. Y. Huang, X. J. Wei, M. Y. Gao, *Chem. Commun.* **2016**, 52, 5872.
- [105] S. W. Yuan, B. Q. Shao, Y. Feng, S. Zhao, J. S. Huo, L. P. Dong, H. P. You, *J. Mater. Chem. C* **2018**, 6, 9208.
- [106] C. S. Lim, A. Aleksandrovsky, M. Molokeev, A. Oreshonkov, V. Atuchin, *J. Solid State Chem.* **2015**, 228, 160.
- [107] K. Z. Zheng, Y. Liu, Z. Y. Liu, Z. Chen, W. P. Qin, *Dalton Trans.* **2013**, 42, 5159.
- [108] S. Wu, W. S. Yu, X. T. Dong, J. X. Wang, G. X. Liu, *Chem. Eng. J.* **2015**, 266, 189.
- [109] M. H. Liu, M. Gu, Y. Tian, P. Huang, L. Wang, Q. F. Shi, C. Cui, *J. Mater. Chem. C* **2017**, 5, 4025.
- [110] I. Rossetti, M. Compagnoni, *Chem. Eng. J.* **2016**, 296, 56.
- [111] F. Qian, *Engineering* **2019**, 5, 981.
- [112] S. Mao, B. Wang, Y. Tang, F. Qian, *Engineering* **2019**, 5, 995.
- [113] J. B. Edel, R. Fortt, J. C. deMello, A. J. deMello, *Chem. Commun.* **2002**, 1136.
- [114] M. X. Jiao, J. F. Zeng, L. H. Jing, C. Y. Liu, M. Y. Gao, *Chem. Mater.* **2015**, 27, 1299.
- [115] Y. Pu, F. H. Cai, D. Wang, J. X. Wang, J. F. Chen, *Ind. Eng. Chem. Res.* **2018**, 57, 1790.
- [116] X. X. Zhu, Q. H. Zhang, Y. G. Li, H. Z. Wang, *J. Mater. Chem.* **2008**, 18, 5060.
- [117] X. X. Zhu, Q. H. Zhang, Y. G. Li, H. Z. Wang, *J. Mater. Chem.* **2010**, 20, 1766.
- [118] D. C. Che, X. X. Zhu, P. F. Liu, Y. R. Duan, H. Z. Wang, Q. H. Zhang, Y. G. Li, *J. Lumin.* **2014**, 153, 369.
- [119] J. R. Burns, C. Ramshaw, *Chem. Eng. Sci.* **1996**, 51, 1347.
- [120] H. Zhao, L. Shao, J.-F. Chen, *Chem. Eng. J.* **2010**, 156, 588.
- [121] Y. Y. Kuang, Z. B. Zhang, M. L. Xie, J. X. Wang, Y. Le, J.-F. Chen, *Ind. Eng. Chem. Res.* **2015**, 54, 8157.
- [122] Y. Pu, L. Lin, J. Liu, J.-X. Wang, D. Wabg, *Chin. J. Chem. Eng.* **2020**, 28, 1744.
- [123] C. C. Lin, Y. J. Chiang, *Chem. Eng. J.* **2012**, 181–182, 196.
- [124] Q. Liu, Y. Pu, Z. Zhao, J.-X. Wang, D. Wang, *Transac. Tianjin Univ.* **2020**, 26, 273.
- [125] S. Lei, J. Chen, *China Particuology* **2005**, 3, 134.
- [126] J.-F. Chen, Y. H. Wang, F. Guo, X. M. Wang, C. Zheng, *Ind. Eng. Chem. Res.* **2000**, 39, 948.
- [127] H. J. Yang, G. W. Chu, J. W. Zhang, Z. G. Shen, J.-F. Chen, *Ind. Eng. Chem. Res.* **2005**, 44, 7730.
- [128] Y. Ouyang, Y. Xiang, H. K. Zou, G. W. Chu, J.-F. Chen, *Chem. Eng. J.* **2017**, 321, 533.
- [129] A. M. Dehkordi, A. Vafaeimanesh, *Ind. Eng. Chem. Res.* **2009**, 48, 7574.
- [130] X. Yin, Q. Sun, D. Wang, A. F. Routh, Y. Le, J. X. Wang, J.-F. Chen, *AIChE J.* **2019**, 65.
- [131] J. N. Leng, J. Y. Chen, D. Wang, J. X. Wang, Y. Pu, J.-F. Chen, *Ind. Eng. Chem. Res.* **2017**, 56, 7977.
- [132] Y. Pu, J. N. Leng, D. Wang, J. X. Wang, N. R. Foster, J.-F. Chen, *Powder Technol.* **2018**, 340, 208.
- [133] Y. Y. Zhan, Y. F. Wan, M. J. Su, Y. Luo, G. W. Chu, L. L. Zhang, J.-F. Chen, *Ind. Eng. Chem. Res.* **2019**, 58, 14588.
- [134] Y. R. Jiao, Y. Pu, J. X. Wang, D. Wang, J.-F. Chen, *Ind. Eng. Chem. Res.* **2019**, 58, 22306.
- [135] M. S. Song, Y. M. Kang, J. H. Kim, H. S. Kim, D. Y. Kim, H. S. Kwon, J. Y. Lee, *J. Power Sources* **2007**, 166, 260.
- [136] A. M. Glushenkov, H. Z. Zhang, J. Zou, G. Q. Lu, Y. Chen, *Nanotechnology* **2007**, 18, 175604.
- [137] J. Zhang, H. Riesen, *Chem. Phys. Lett.* **2015**, 641, 1.
- [138] Z. Q. Liu, M. A. Stevens-Kalceff, X. L. Wang, H. Riesen, *Chem. Phys. Lett.* **2013**, 588, 193.
- [139] J. Zhang, N. Riesen, H. Riesen, *Nanoscale* **2017**, 9, 15958.
- [140] H. K. Yang, J. H. Jeong, *J. Phys. Chem. C* **2010**, 114, 226.



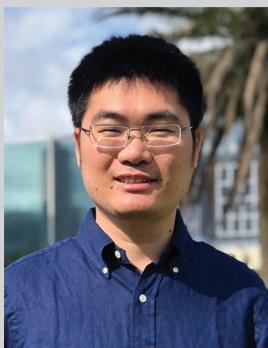
**Yiran Jiao** received a B.E. degree in chemical engineering and technology from East China University of Science and Technology, Shanghai, China, in 2017. He then received a masters degree in chemical engineering and technology at the Beijing University of Chemical Technology, Beijing, China, in 2020. His research focuses on process intensification technology for optical nanomaterials and applications.



**Ben Bin Xu** is a professor of materials and mechanics in the Department of Mechanical and Construction Engineering at Northumbria University, United Kingdom. Dr. Xu obtained his M.Sc. in materials science (2006) and B.Eng. (H) in polymer science (2003) from Zhejiang University of Technology in China. After completing a Ph.D. in mechanical engineering (2011) at Heriot-Watt University in Edinburgh, Ben moved to the University of Massachusetts, Amherst (US), to work (2011-2013) with Prof. Ryan C. Hayward as a postdoc research fellow in polymer science and engineering. Dr. Xu's research interests include responsive materials, materials chemistry and physics, soft matter, applied mechanics, and micro-engineering.



**Steven Wang** is an assistant professor in the Department of Mechanical Engineering at City University of Hong Kong. He was a faculty member (2016-2019) at Newcastle University, United Kingdom before joining the faculty of City University of Hong Kong. Dr. Wang received B.E. degree in chemical engineering from the University of Melbourne and Ph.D. in chemical engineering from Monash University. He specializes in fluid/applied mechanics, applied surfaces, and energy.



**Dan Wang** is a professor at College of Chemical Engineering in Beijing University of Chemical Technology, Beijing, China. He received B.E. degree and Ph.D. degree from Zhejiang University in 2008 and 2013, respectively. His research interests focus on optical nanomaterials and devices. Dr. Wang was visiting scholar at Harvard University (2019), Case Western Reserve University (2013-2015).